RSC Advances




ROYAL SOCIETY OF CHEMISTRY

www.rsc.org/advances

Journal Name

RSCPublishing

ARTICLE

# cRGD targeted and charge conversion-controlled release micelles for doxorubicin delivery

Cite this: DOI: 10.1039/x0xx00000x

Xingang Guan,[a,b] Xiuli Hu,[a] Zhihong Li,[c] Hong Zhang*[c] and Zhigang Xie*[,a]

Received 00th January 2012,
Accepted 00th January 2012

DOI: 10.1039/x0xx00000x

www.rsc.org/

Efficiently and selectively delivering chemotherapeutic agents to tumours still remains a challenge for development of nanocarriers. In this study, polymer micelles based on cRGD targeting and pH-sensitive surface charge switching were successfully prepared and used for doxorubicin (Dox) delivery. This nanoscale polymeric micelle indicated high drug encapsulation efficiency of 90% and slight negative charge. Drug release experiment showed the pH-enhanced release profile in PBS, which resulted from surface charge switching imidazole. Confocal laser scanning microscopy and flow cytometry experiments indicated that combining the capability of RGD-target and pH-sensitive charge switching significantly enhanced cellular uptake of B16F10 cells overexpressing $\alpha_v\beta_3$ integrins. MTT assay also showed that our hybrid micelles were much more cytotoxic to B16F10 cells than other micelles. These results suggest the potential application of cRGD target and pH-sensitive surface charge switching polymeric micelles in the treatment of $\alpha_v\beta_3$ integrins-overexpressing cancers.

## 1 Introduction

Nowadays, great progress have been made in understanding the mechanism of tumor origination and development, however, surgery, chemotherapy and radiation still represent as the main methods for current cancer treatments.[1, 2] Although traditional chemotherapeutic agents could remarkably suppress the tumor growth, their application was greatly hindered by the side effects to normal cells. Delivering the anti-cancer agents to tumor cells without releasing in normal cells is the primary question in development of efficient anti-tumor carriers. Nanomedicines, drugs based on nanotechnology, hold great promise to improve the outcome of chemotherapy.[3-9] Drug-delivery systems (DDSs) based on engineered nanoparticles possess many advantages such as the reduced cytotoxicity, enhanced permeability and retention effect (EPR effect),[10, 11] responsive property to tumor microenvironment (*e.g.*, pH, redox, enzymes or others),[12-15] increased cell uptake by equipping target moiety (*e.g.* peptides, antibodies, and aptamers).[16-18]

It is well-known that the pH value in tumor extracellular environment is much lower (pH 5.8–6.5) than that in blood (pH 7.4),[19-21] and even much lower pH values (pH 5.0–5.5) were detected in intracellular organelles (e.g., late endosomes and lysosomes ).[22]Accumulating reports indicated that many types of pH-sensitive nanoparticles have been developed and efficiently delivered their payload to the tumor environment.[23-26] These pH-responsive nanocarriers could preserve the stable conformation or keep the integrity of pH-sensitive linkages under the physiological pH; however, when the nanocarriers were transported across the super-permeabilized vasculture to the tumor stroma (low pH) via EPR effect, the breakage of pH-sensitive conformation or linkages will release the drugs to tumor extracellular environment. Recently, many reports suggested that charge-conversion was proved to be a good method to improve the efficiency of drug delivery to tumor cells.[27-29] The utilization of 1-(3-aminopropyl) imidazole (API) in mediating the pH-responsive charge-switching via the protonation finally leads to enhanced drug accumulation in tumor cells. However, the drug accumulation of tumor cells in most studies mainly relied on the EPR effect, which is not enough to improve the tumor cell uptake significantly. Target delivery of anti-tumor agents is considered to open a new era for chemotherapy of cancers. By decoration of target ligands on the surface of nanocarriers, these drug nanocarriers could selectively bind with the corresponding receptors highly or uniquely expressed on tumor cells and then be internalized via endocytosis.[30-32] DDS based on active targeting has been proved to significantly improve the therapeutic efficacy of

tumors. Among various target ligands, RGD peptide was preferentially used due to its low cost and high expression of its receptors ($\alpha_v\beta_3$ and $\alpha_v\beta_5$ integrins) in many solid tumors and tumor vasculture endothelial cells.[33, 34]. Accumulating studies have indicated the key role of RGD peptides in target delivery of various nanoparticles to tumor cells overexpressing $\alpha_v\beta_3$ or $\alpha_v\beta_5$ integrins.[35-44]

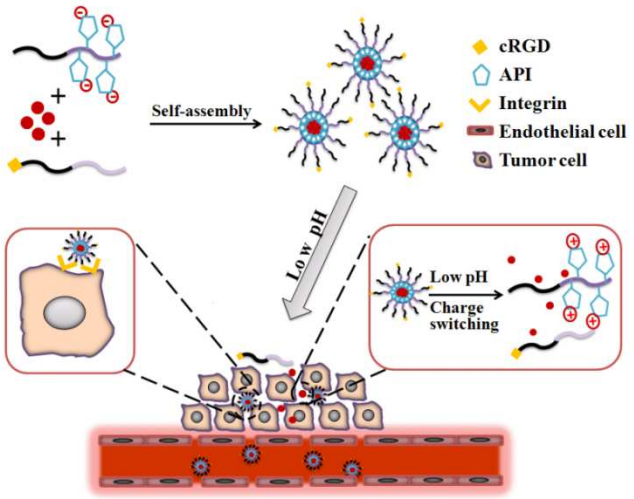


**Scheme 1** Schematic illustration of self-assembly and tumor cell uptake of cRGD target, pH-triggered surface charge-switching polymer micelles.

In this study, to develop DDS with excellent biocompatibility, polymer micelles based on poly (ethylene glycol)-block-poly (glutamic acid) were successfully synthesized. Poly (glutamic acid) was chosen as backbone polymer not only for its excellent biocompatibility and biodegradability, but also for its abundant functional carboxyl groups which was convenient for conjugating.[45,46] By conjugation of API on the side chains, polymer micelle with pH-responsive charge switching property was prepared. By decoration with c(RGDfK) peptide, our charge conversion micelles were used to deliver doxorubicin (Dox) to mouse melanoma cells. Drug release profile in vitro, cellular uptake and cytotoxicity analysis were evaluated in detail.

## 2 Material and Methods

### 2.1 Materials

Monomethoxylpoly(ethylene glycol) (mPEG, average Mn=5000), dicyclohexylcarbodiimide (DCC, 99%) and N-hydroxysuccinimide (NHS, 99%) were purchased from Aldrich (USA). N-(3-Aminopropyl)-imidazole (API) was ordered from Alfa Aesar. Doxrobicin (Dox) was purchased from Zhejiang Hisun Pharmaceutical Co. Ltd (Taizhou city, China). 4',6-diamidino-2-phenylindole (DAPI) was purchased from Shanghai Yuanye Ltd (Shanghai, China). MTT (3-[4,5-dimethylthiazol-2-yl]-2,5-diphenyltetrazolium bromide) and 9,10-phenan-threnequinone were purchased from Amresco (USA). cyclic (RGDfK) peptide was customized from Shanghai China peptides Ltd (Shanghai, China). Ultrapure water was prepared from a Milli-Q system (Millipore, USA). All other chemicals were analytical grade or above.

### 2.2 Synthesis of PEG-PGlu$_{10}$

Poly(ethylene glycol)-poly (glutamic acid) (PEG-P(Glu)) block copolymers were synthesized by the previously reported synthetic method with a little modification.[47] Ring opening polymerization of the *N*-carboxy anhydride of β-benzyl L-glutamate was carried out using mPEG-$NH_2$ as macroinitiator. Briefly, in a dried flask, 5.0 g of PEG-$NH_2$ (1.0 mmol) and 2.63 g of BGL-NCA (10 mmol) were dissolved in dried chloroform (65 mL), and the solution was stirred for 72 h at 30$^o$C. The product mixture was precipitated with an excess of a mixture of acetic acid and methanol (1:3, v/v) under vigorous stirring to give a white solid. PEG-PBGL was obtained under vacuum at 40$^o$C for 24 h.

In order to remove the protected benzyl group, mPEG-b-P(BLG$_{10}$) (3.0 g) was dissolved in dichloro acetic acid (30 mL) and HBr/acetic acid (33 wt%, 12 mL) was added. After stirring for 1 h at 35$^o$C, the mixture was precipitated into excessive ice diethyl ether. After drying under vacuum, the precipitate was dissolved in DMF and dialyzed against distilled water, and then freeze-dried to give PEG-PGlu$_{10}$ product. The $^1$H NMR spectra of the protected and unprotected PEG-PGlu$_{10}$ are given in Fig. 1.

### 2.3 Synthesis of PEG-PGA$_{10}$-API

PEG-PGA$_{10}$ (200 mg, 25 μmol) was dissolved in 5ml DMSO, then 7.74mg dicyclohexylcarbodiimide (DCC) (37.5 μmol) and 4.32 mg N-hydroxysuccinimide (NHS) (37.5 μmol) were added. The reactions were conducted at room temperature for 2 hours and then N-(3-Aminopropyl)-imidazole (API) (16 mg, 125 μmol) was added. After dialysis against distilled water for 12 hours (MWCO=3500), the final suspension in dialysis bag was freeze-dried.

### 2.4 Synthesis of cRGD-PEG-PLA

cRGD-PEG-PLA was synthesized in previous work.[26]

### 2.5 Preparation of Dox-loaded micelles M(Dox) and RGD-M(Dox)

M(Dox) micelles were prepared as follows: 4 mg Dox-HCl, 36 mg PEG-PGA$_{10}$-API and 20 μL triethylamine (TEA) were dissolved in 2 mL DMSO, the mixed solution was drop wise added to 10 mL deionized water. Unloaded Dox and DMSO was removed by dialysis against distilled water for 8 hours (MWCO=3500). The Dox-loaded micelles were stored at 4$^o$C and used within one month. When M(Dox) micelles was used in target analysis compared with RGD-M(Dox) which contains 20% cRGD-PEG-PLA, M(Dox) micelles were prepared by mixing 4 mg Dox-HCl, 28.8 mg PEG-PGA$_{10}$-API and 7.2 mg PEG-PLA, other process were same to above.

RGD-M(Dox) were prepared by mixing PEG-PGA$_{10}$-API and cRGD-PEG-PLA with weight ratio and 20/80, that is to say a mixture of 4 mg Dox-HCl, 28.8 mg PEG-PGA$_{10}$-API and 7.2 mg cRGD-PEG-PLA were used as the starting materials.

The loading content of Dox was determined by the UV absorbance at 480 nm, according to the standard calibration

curve of free Dox in DMSO. Briefly, free Dox solution in DMSO was used to construct standard curve. Then the freeze-dried Dox-loaded micelles were weighed and dissolved in DMSO, the absorbance of which at 480 nm was measured. The Dox content can be acquired according to the standard curve. Drug Loading Content (DLC) and drug loading efficiency (DLE) was calculated according to the following equation:

DLC%= (weight of Dox in the micelle/weight of Dox + weight of all polymers) ×100%

DLE%= (weight of Dox in the micelle/weight of Dox added) ×100%

**2.6 Characterization of M(Dox) and RGD-M(Dox)**

The morphology of polymer micelles was determined by transmission electron microscope (TEM) (JEOL JEM-1011 electron microscope). Size distribution of micelles was measured by dynamic light scattering (DLS) with a vertically polarized He–Ne laser (DAWN EOS, Wyatt Technologies). The scattering angle was fixed at 90° for DLS measurement at 25℃.

**2.7 Dox release in vitro**

The release profile of Dox from M(Dox) were studied at 37°C in PBS buffers of different pH values (pH 5.8, pH 6.5 and pH 7.4). Briefly, micelle dispersion containing 1 mg EPI was transferred into dialysis bag (MWCO=3000) followed by immersing in 20 ml PBS buffer (20 mM, pH 5.8, pH 6.5 and pH 7.4) with stirring at 37°C. At certain time points, 1 ml dialysis solution was taken out for UV-Vis measurement (480 nm) and replenished with 1 ml fresh PBS solution.

**2.8 Biocompatibility assay of polymers**

In this study, a cancer cells (B16F10 cells, originated from mouse skin melanoma) and a non-cancer cell (L929 cells, mouse fibroblast cells) were used to examine the biocompatibility of polymers. After 5 times of passaging, cells were seeded in 96-well plates at a density of $4\times10^3$cells/well in 100 μL Dulbecco's modified Eagle's medium (DMEM) containing 10 % fetal bovine serum (FBS) for 12 h at 37 $^oC$ in 5 % $CO_2$. The medium was replaced with 200 μl DMEM medium containing different concentrations of PEG-$PGA_{10}$ (ranging from 100 to 1000 μg/ml) and PEG-$PGA_{10}$-API (ranging from 50 to 500 μg/ml) for 48 h. 20 μl MTT (5 mg/ml) was added to each well for 4 h incubation, and then 150 μl DMSO were added to each well to dissolve the blue formazan formed in the live cells. The absorbance was measured on a microplate reader (BioTek, EXL808) at 490 nm. Experiments were repeated three times.

**2.9 The cytotoxicity analysis of M(Dox) and RGD-M(Dox)**

The cytotoxicity of two types of Dox-loaded micelles was measured via MTT assay with free Dox as a control. Briefly, B16F10 melanoma cells were seeded in 96-well plates at $2\times10^3$ cells/well with drugs in 100 μL DMEM medium containing 10% fetal bovine serum (FBS) for 12 h of incubation at 37 $^oC$ in 5% $CO_2$.The medium was replaced with 200 μl DMEM medium containing different concentrations of Dox or micelles (ranging from 0.01 to 10 μg/ml ) for 48 h. 20 μl MTT (5 mg/ml in PBS buffer) was added to each well for 4 h of incubation, and then 150 μl DMSO were added to each well to dissolve the blue formazan formed in the live cells. The absorbance was measured on a microplate reader (BioTek, EXL808) at 490 nm. Experiments were repeated three times.

**2.10 The Cellular uptake study**

The cellular uptake of M(Dox) and RGD-M(Dox) was evaluated by confocal laser scanning microscopy(CLSM) and flow cytometry.

For CLSM analysis, B16F10 cells were seeded into a six-well plate at a density of $4\times10^5$ cells perwell for 12 h incubation. The medium was replaced with fresh DMEM medium containing Dox or micelles (containing equal Dox, 20 μg/ml) for 1 h. After three times of washing with PBS, the cells were fixed with 4% (w/v) paraformaldehyde for 10 min at room temperature. The cell nuclei were stained with DAPI (6-diamidino-2-phenylindole) for 15 min. CLSM images were captured via confocal microscope (Carl Zeiss LSM 780) under the same conditions. The mean fluorescence intensity of each cell was analyzed by Image Pro-Plus (IPP) software according to the inherent fluorescence of Dox. As for A549 carcinoma cells (a human cell line derived from the respiratory epithelium) uptake, the process was same to that of B16F10 cells.

For flow cytometry, the cell seed and drug incubation process was same to that in CLSM. The cells were treated with 200 μl 0.25% trypsin for 2 min. After adding 1 ml DMEM medium, the cells were centrifuged at 300 × g for 5 min. After removing supernatant, the cells were resuspended in 0.5 ml PBS. Flow cytometry analysis was performed by a flow cytometer (Beckman, USA) which collected $1\times10^4$gated events for each sample.

**2.11 Statistics**

All experiments were performed at least three times and all results are expressed as mean±SD (standard deviation). Students't-test was used to demonstrate statistical significance ($P<0.05$).

**3. Results and discussion**

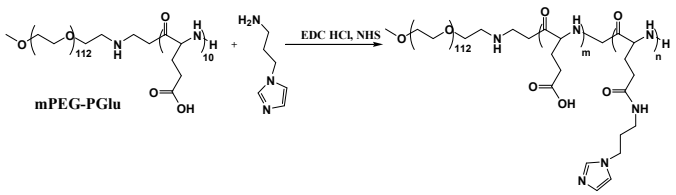


**Scheme 2** Synthetic routes for preparation of PEG-PGA-API.

**3.1 Preparation and characterization of M(Dox) and RGD-M(Dox)**

First, amphiphilic copolymer PEG-PGA-API was made through the amidation of mPEG-PGlu with API in the presence of

EDC/NHS as shown in Scheme 2. The chemical structure was characterized by $^1$H NMR. As shown in Fig. 2, the presence of imidazole was confirmed by the characteristic signals at 6.9, 7.2 and 7.6 ppm. The content of API in PEG-PGA-API calculated by the intensity of $^1$H NMR is about 5 wt%. Then the conjugation of cRGD on to PEG-PLA was done and confirmed according to the literature.[26,48] The molar ratio of cRGD to PEG-PLA was determined to 1:1.06 calculated by standard curve. That means that average 94% of polymer was labelled by cRGD.

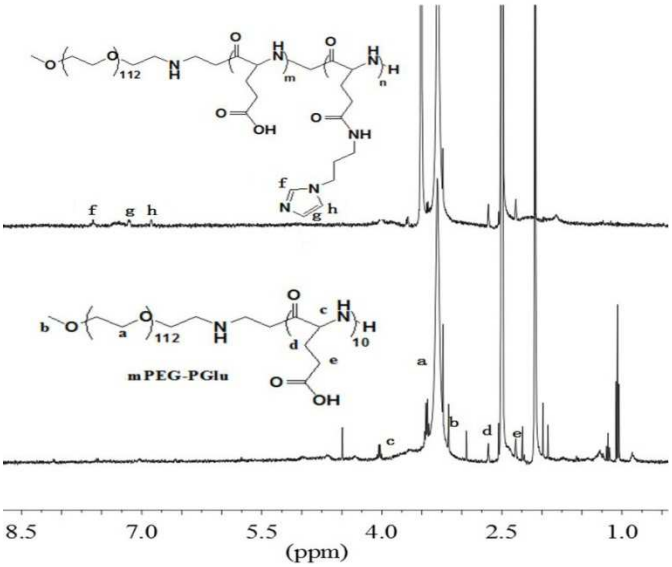


**Fig. 1** The $^1$H NMR spectra of PEG-PGA and PEG-PGA-API

**Table 1** Characterizations of micelles.

| Micelles | Size (nm) | PDI | Zeta Potential (mV) | Drug Loading Content (DLC) % | Drug Loading Efficiency (DLE) % |
|---|---|---|---|---|---|
| M(Dox) | 26.42±1.72 | 0.399 | -18.8±1.41 | 8.73 | 87.25 |
| cRGD-M(Dox) | 30.12±1.83 | 0.439 | -4.42±1.07 | 8.72 | 86.13 |

The amphiphilic block could self-assembly into polymeric micelles in aqueous solution. Herein, the Dox-loaded micelles prepared with PEG-PGA-API were named M(Dox). The hybrid micelles containing cRGD decoration named RGD-M(Dox) were prepared using the co-assembly method. Considering the good target ability of 20% cRGD described by Miura Y,[37] cRGD target micelles were prepared by using a mixture of cRGD-PEG-b-PLA and PEG-PGA-API- in the ratio of 1:4 in this study. The characterizations of two micelles were shown in Table 1. The average diameters of M(Dox) and RGD-M(Dox) were 26 nm and 30 nm respectively. The increase in diameter of RGD-M(Dox) could be attribute to the cRGD decoration on the surface of micelles. The zeta potential of M(Dox) and RGD-M(Dox) was -18.8 and -4.4 respectively. TEM analysis indicated that both micelles displayed nearly sphere nanosized structure (shown in Fig. 2A). Two micelles showed nearly same drug loading capability, (DLC 8.7%, DLE 86%~88%), indicating the nearly ignored effect of cRGD decoration in loading drugs. The charge conversion property of two micelles conferred by imidazole were also analyzed in PBS buffer with different pH values. As shown in Fig. 2B, M(Dox) and RGD-M(Dox) micelles had negative charge; when two micelles was immersed in acidic environment, the micelles surface converted to positive charge within 4h, suggesting the important role of imidazole in surface conversion.

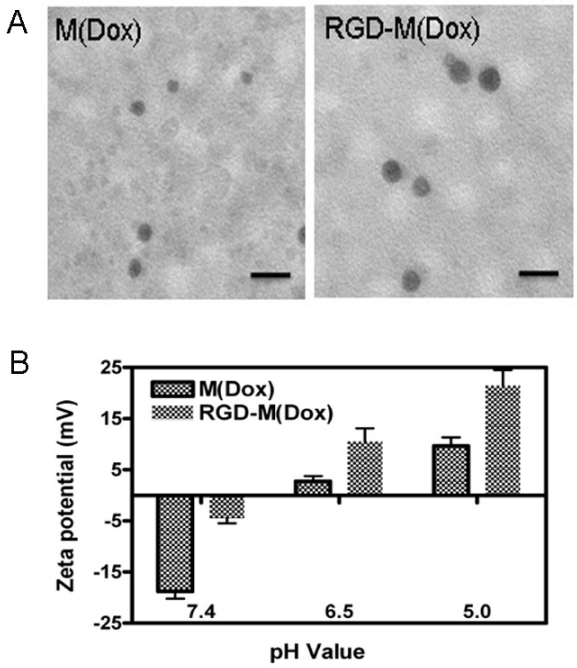


**Fig. 2** TEM analysis (A) and surface charge conversion of M(Dox) and RGD-M(Dox) in different pH values. Scale bar was equal to 50 nm.

The release of EPI from micelles was determined in PBS buffer (pH 5.8, pH 6.5 and pH 7.4), respectively. The results (Fig. 3) showed that both M(Dox) and RGD-M(Dox) exhibited a sustained-release in three types of PBS. Compared with micelles, free Dox displayed a fast release in pH7.4 and pH5.0 PBS; the cumulative release can reach about 76.8% after 4h of release. After 36 h of release, the cumulative Dox release in pH 5.8, pH 6.5 and pH 7.4 PBS were 80.3%, 57.0% and 45.4%, respectively; as for RGD-decorated micelles, the cumulative Dox release in the same PBS 43.4%, 56.1%, and 80.8%. The enhanced Dox release from M(Dox) and RGD-M(Dox) micelles suggested pH-sensitive property. The result could be attributed to the pH-responsive imidazole groups in micelles. No significant difference in cumulative Dox release (after 36h) was detected between M(Dox) and RGD-M(Dox) micelles when in same PBS buffer.

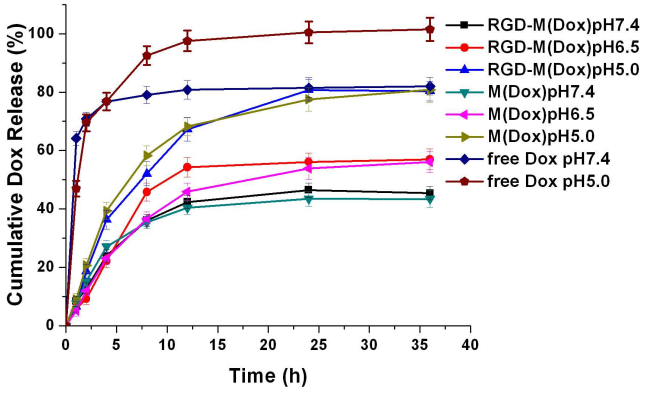

**Fig. 3** Cumulative release profiles of Dox from free Dox, M(Dox) and RGD-M(Dox) in vitro at different pHs (pH 5.8, 6.5 and 7.4) at 37℃.

### 3.2 Biocompatibility study of M(Dox) and RGD-M(Dox)

To evaluate if our micelles could be used for drug delivery, the biocompatibility of block copolymer PEG-PGA and PEG-PGA-API were investigated by MTT assay. PEG-PGA showed perfect biocompatibily at concentrations up to 1 mg/mL (>90%), and PEG-PGA-API also suggested low cytotoxicity at concentrations up to 500 μg/mL (>80%) (shown in Fig. 4). The slightly reduced biocompatibility of PEG-PGA-API may be ascribed to the introduction of API.

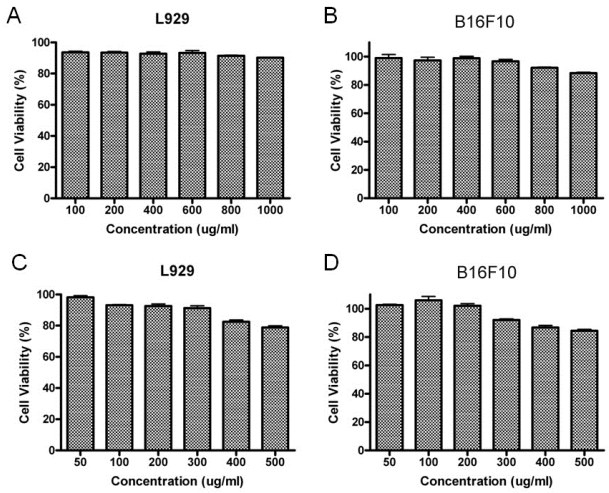


**Fig. 4** Cell viability of L929 and B16F10 cells treated with PEG-PGA (A, C) and PEG-PGA-API (B, D) at different concentration after 48 h incubation at 37 °C. All the results were repeated three times, and presented as mean±SD.

### 3.3 Cellular uptake

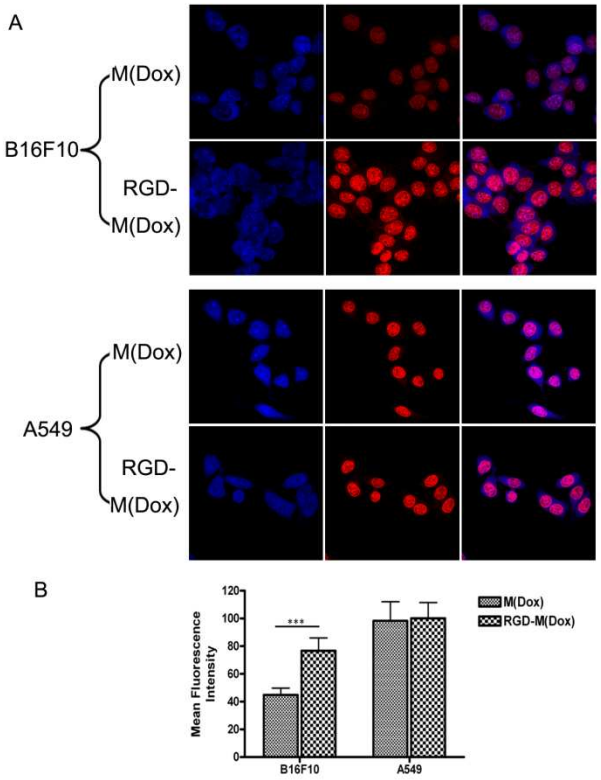


**Fig. 5** CLSM images of B16F10 cells and A549 cells treated with M(Dox) and RGD-M(Dox) at pH 7.4 PBS after 1 h of incubation at 37℃ in vitro (A); the quantification of mean fluorescence intensity of each cell were also shown (B).

To evaluate the target ability of cRGD-decorated micelles, the cellular uptake of M(Dox) and RGD-M(Dox) by B16F10 and A549 cells were studied according to the inherent fluorescence of Dox. B16F10 cells express high level of $\alpha_v\beta_3$ integrins, whereas nearly no expression in A549 cells, as described in many literatures.[26]

As shown in Fig. 5A, all cells displayed strong red fluorescence in the cell nucleus, and little fluorescence was distribute in cytosol. Moreover, cRGD-decorated micelles showed much higher red fluorescence in nucleus than undecorated micelles in B16F10 cells, while no obvious change was observed in the fluorescence intensity of two micelles in A549 cells (Fig. 5A). The quantification analysis of mean fluorescence intensity confirmed our conclusion (Fig. 5B). This result indicated that RGD decoration significantly improved the endocytosis of B16F10 cell overexpressed $\alpha_v\beta_3$ integrins. Due to the very low expression of $\alpha_v\beta_3$ integrins in A549 cells, the significantly enhanced endocytosis of RGD-decorated micells was not observed. The more cellular uptake of M(Dox) micelles by A549 cells than B16F10 cells may be attributed to different cell sources, that is to say, the cell uptake of micelles by respiratory epithelium cells (A549 cells) seems to be much easier than that in skin cells (B16F10 cells).

Based on the target result, micelles combining cRGD decoration and charge switching imidazole group were developed with the cRGD-PEG-PLA and PEG-PGA-API at the ratio of 1:4 (wt/wt). Considering the RGD content in the copolymer of cRGD-PEG-PLA was 94%, the real RGD content in RGD-M(Dox) micelles was calculated to 18.8%. The cellular uptake of M(Dox) and RGD-M(Dox) in PBS (pH 7.4 and pH 5.8) were investigated on B16F10 cells. As shown in Fig. 6A and 6B, the RGD-M(Dox) micelles in pH 7.4 PBS (abbreviated as RGD-M/7.4) and M(Dox) in pH 5.8 PBS (abbreviated as M/5.8) showed much stronger fluorescence than M(Dox) in pH7.4 PBS, which may be ascribed to the cRGD decoration and imidazole group; moreover, the cells treated with RGD-M(Dox) micelles in pH 5.8 PBS (abbreviated as RGD-M/5.8) showed more higher fluorescence than other three groups, indicating a synergy effect of cRGD decoration and imidazole in improving cell uptake. The cell uptake was also examined by flow cytometric analysis. The results of flow cytometric experiments supported the CLSM results (Fig. 7). In acidic environment the cell uptake rate increased from 27.6% in pH 7.4 to 40.1%, which could be interpreted as the drug fast release caused by charge switching of imidazole; and after cRGD decoration, the cell uptake rate was raised to 55.7%, that may be attribute to the increased endocytosis by B16F10 cells mediated by cRGD decoration. When combining cRGD target and acidic environment, this group showed the highest cell uptake rate in four groups (77.2%), just as the result in CLSM experiments.

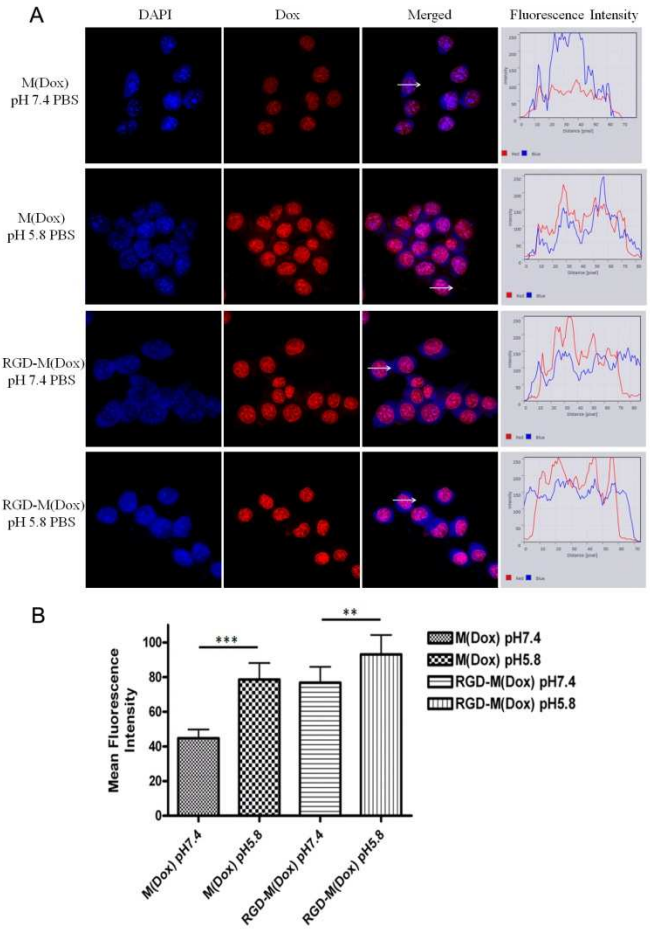


**Fig. 6** CLSM images of B16F10 cells treated with M(Dox) and RGD-M(Dox) at pH 7.4 and pH 5.8 PBS after 1 h of incubation at 37 ℃ in vitro respectively (A); the mean fluorescence intensity of Dox of each cell were also shown (B).

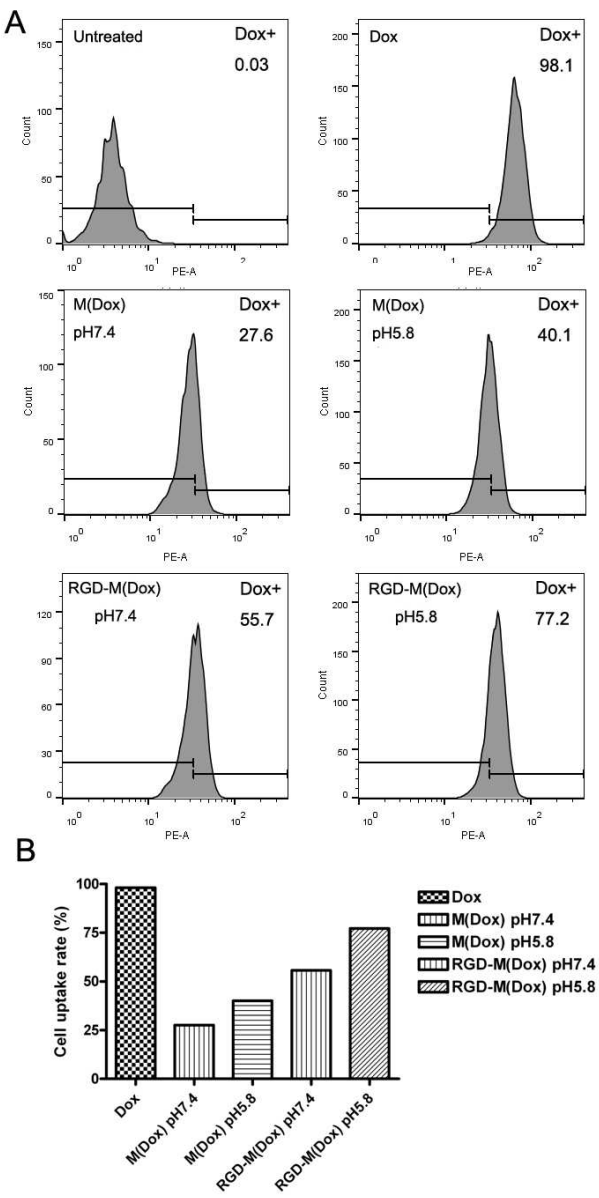


**Fig. 7** Flow cytometry analysis of B16F10 cells treated with M(Dox) and RGD-M(Dox) at pH 7.4 and pH 5.8 PBS after 1 h of incubation at 37℃, Dox as a positive control (A); cell uptake rate of B16F10 cells were shown (B).

### 3.4 Cytotoxicity analysis

Base on the significantly improved cellular uptake results, we expected that our hybrid micelles could kill more cells than undecorated. The cytotoxicity of Dox-loaded micelles was evaluated by MTT assay. The cell viability of B16F10 cells incubated with Dox, M(Dox) and RGD-M(Dox) for 48 h at the indicated Dox concentration. As shown in Fig.7, the cell viability showed a dose-dependent manner for three types of Dox formulation. Free Dox shows the best cytotoxicity against B16F10 cells among three Dox formulations, which could be attributed to more cellular uptake than two micelles (shown in Fig. 6A). The cell viability at each concentration followed the order of Dox< RGD-M(Dox)<M(Dox), suggesting the lower cytotoxicity of M(Dox) than RGD-M(Dox). RGD-decorated micelles displayed much more endocytosis by B16F10 celles than undecorated micelles determined by flow cytometry analysis, which directly led to the more nuclear Dox accumulation indicated by CLSM. So RGD-M(Dox) micelles killed more cells than M(Dox) micelles, suggesting a higher cytotoxicity of RGD-decorated micelles.

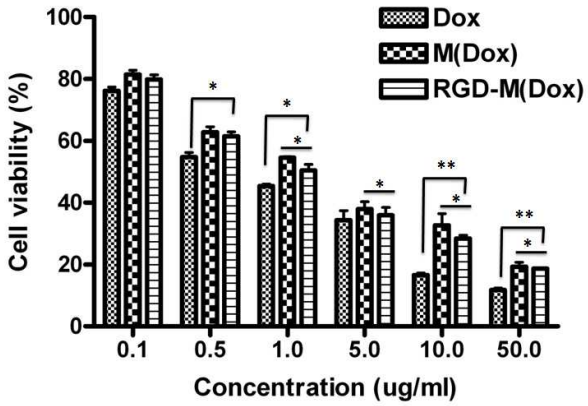


**Fig. 7** The cytotoxicity analysis of B16F10 cells treated with M(Dox) and RGD-M(Dox) after 48 h of incubation at 37℃. All the results were repeated three times, and presented as mean±SD.

## 4 Conclusion

In summary, we successfully developed Dox-loaded micelles combining cRGD targeting and charge conversion function. The micelles showed a hydrodynamic diameterof 30.1 nm, -4.42 mV of zeta potential, and almost 90% of drug encapsulation efficiency. The Dox-loaded micelles exhibited a sustained, low pH-enhanced release profile in PBS. CLSM and flow cytometry analysis indicated significantly improved cellular uptake, mediating by selective binding of RGD to $\alpha_v\beta_3$ integrins and pH-triggered surface charge switching. Our results *in vitro* demonstrated the key roles of combining RGD decoration and imidazoles in improving delivery of anti-cancer agents to some tumours overexpressing $\alpha_v\beta_3$ integrins, which may be used to develop efficient drug delivery system for cancer therapy in the future.

## Acknowledgements

The project was supported by the National Natural Science Foundation of China (Project No. 91227118 and 51373167).

## Notes and references

[a]*State Key Laboratory of Polymer Physics and Chemistry, Changchun Institute of Applied Chemistry, Chinese Academy of Sciences, 5625 Renmin Street, Changchun 130022, P. R. China*
*E-mail: xiez@ciac.ac.cn; Tel/fax: +86-431-85262775*

[b]*Life Science Research Center, Beihua University, Jilin 132013, P. R. China*
[c]*Department of Thoracic Surgery, The first Hospital of Jilin University, Changchun 130021, P. R. China. E-mail: yveszhang@hotmail.com*

1 S. D. Steichen, M. Caldorera-Moore and N. A. Peppas, *Eur. J. Pharm. Sci*, 2013, **48**, 416-427.
2 F. Alexis, E. M. Pridgen, R. Langer and O. C. Farokhzad, in *Drug Delivery*, Springer, 2010, pp. 55-86.
3 Z. Cheng, A. Al Zaki, J. Z. Hui, V. R. Muzykantov and A. Tsourkas, *Science*, 2012, **338**, 903-910.
4 P. Couvreur, *Adv Drug Deliver. Rev*, 2013, **65**, 21-23.
5 K. Kataoka, A. Harada and Y. Nagasaki, *Adv Drug Deliver. Rev*, 2011, **47**, 113-131.
6 D. Peer, J. M. Karp, S. Hong, O. C. Farokhzad, R. Margalit and R. Langer, *Nat. Nano*, 2007, **2**, 751-760.
7 X. Hu and X. Jing, *Expert Opin. Drug Del*, 2009, **6**, 1079-1090.
8 X. Hu, J. Li, W. Lin, Y. Huang, X. Jing and Z. Xie, *RSC Advances*, 2014, **4**, 38405-38411.
9 X. Hu, S. Liu, Y. Huang, X. Chen and X. Jing, *Biomacromolecules*, 2010, **11**, 2094-2102.
10 E. K.-H. Chow and D. Ho, *Sci. Transl. Med*, 2013, **5,** 216rv214-216rv214.
11 H. Maeda, *Adv. Enzyme Regul*, 2001, **41**, 189-207.
12 E. S. Lee, K. Na and Y. H. Bae, *Nano Lett*, 2005, **5**, 325-329.
13 D. Ling, W. Park, S.-j. Park, Y. Lu, K. S. Kim, M. J. Hackett, B. H. Kim, H. Yim, Y. S. Jeon, K. Na and T. Hyeon, *J. Am. Chem. Soc*, 2014, **136**, 5647-5655.
14 X. Yang, J. J. Grailer, I. J. Rowland, A. Javadi, S. A. Hurley, V. Z. Matson, D. A. Steeber and S. Gong, *ACS Nano*, 2010, **4**, 6805-6817.
15 M. S. Muthu, C. V. Rajesh, A. Mishra and S. Singh, *Nanomedicine*, 2009, **4**, 657-667.
16 R. Wang, X. Hu, S. Wu, H. Xiao, H. Cai, Z. Xie, Y. Huang and X. Jing, *Mol. Pharmaceut*, 2012, **9**, 3200-3208.
17 T. M. Allen, *Nat. Rev. Cancer*, 2002, **2**, 750-763.
18 L. Brannon-Peppas and J. O. Blanchette, *Adv Drug Deliver. Rev*, 2012, **64, Supplement**, 206-212.
19 J. W. Nichols and Y. H. Bae, *Nano Today*, 2012, **7**, 606-618.
20 O. Trédan, C. M. Galmarini, K. Patel and I. F. Tannock, *JNCI-J. Natl. Cancer I*, 2007, **99**, 1441-1454.
21 F. A. Gallagher, M. I. Kettunen, S. E. Day, D. E. Hu, J. H. Ardenkjaer-Larsen, R. Zandt, P. R. Jensen, M. Karlsson, K. Golman, M. H. Lerche and K. M. Brindle, *Nature*, 2008, **453**, 940-943.
22 Y. Urano, D. Asanuma, Y. Hama, Y. Koyama, T. Barrett, M. Kamiya, T. Nagano, T. Watanabe, A. Hasegawa, P. L. Choyke and H. Kobayashi, *Nat. Med*, 2009, **15**, 104-109.
23 W. She, N. Li, K. Luo, C. Guo, G. Wang, Y. Geng and Z. Gu, *Biomaterials*, 2013, **34**, 2252-2264.
24 H. Wang, F. Xu, D. Li, X. Liu, Q. Jin and J. Ji, *Polym. Chem-UK*, 2013, **4**, 2004-2010.
25 M. Curcio, I. Altimari, U. G. Spizzirri, G. Cirillo, O. Vittorio, F. Puoci, N. Picci and F. Iemma, *J. Nanopart. Res*, 2013, **15**, 1-11.
26 X. Guan, X. Hu, S. Liu, Y. Huang, X. Jing and Z. Xie, *RSC Advances*, 2014, **4**, 55187-55194.
27 X. Hu, X. Guan, J. Li, Q. Pei, M. Liu, Z. Xie and X. Jing, *Chem. Commun*, 2014.
28 D. Ling, H. Xia, W. Park, M. J. Hackett, C. Song, K. Na, K. M. Hui and T. Hyeon, *ACS Nano*, 2014, **8**, 8027-8039.
29 C.-S. Lee, W. Park, Y. U. Jo and K. Na, *Chem. Commun*, 2014, **50**, 4354-4357.
30. J. Yue, S. Liu, R. Wang, X. Hu, Z. Xie, Y. Huang and X. Jing, *Mol. Pharmaceut*, 2012, **9**, 1919-1931.
31 R. Wang, X. Hu, J. Yue, W. Zhang, L. Cai, Z. Xie, Y. Huang and X. Jing, *J. Mater. Chem. B*, 2013, **1**, 293-301.
32 X. Hu, R. Wang, J. Yue, S. Liu, Z. Xie and X. Jing, *J. Mater. Chem*, 2012, **22**, 13303-13310.
33 K. Temming, R. M. Schiffelers, G. Molema and R. J. Kok, *Drug Resist. Updat*, 2005, **8**, 381-402.
34 N. Yonenaga, E. Kenjo, T. Asai, A. Tsuruta, K. Shimizu, T. Dewa, M. Nango and N. Oku, *J. Control. Release*, 2012, **160**, 177-181.
35 J. Yang, Y. Hou, G. Ji, Z. Song, Y. Liu, G. Dai, Y. Zhang and J. Chen, *Eur. J. Pharm. Sci*, 2014, **52**, 180-190.
36 Z. Zhen, W. Tang, H. Chen, X. Lin, T. Todd, G. Wang, T. Cowger, X. Chen and J. Xie, *ACS Nano*, 2013, **7**, 4830-4837.
37 Y. Miura, T. Takenaka, K. Toh, S. Wu, H. Nishihara, M. R. Kano, Y. Ino, T. Nomoto, Y. Matsumoto and H. Koyama, *ACS Nano*, 2013, **7**, 8583-8592.
38 W. Song, Z. Tang, D. Zhang, Y. Zhang, H. Yu, M. Li, S. Lv, H. Sun, M. Deng and X. Chen, *Biomaterials*, 2014, **35**, 3005-3014.
39 F. Danhier, B. Vroman, N. Lecouturier, N. Crokart, V. Pourcelle, H. Freichels, C. Jerome, J. Marchand-Brynaert, O. Feron and V. Preat, *J. Control. Release*, 2009, **140**, 166-173.
40 H. Tian, L. Lin, J. Chen, X. Chen, T. G. Park and A. Maruyama, *J. Control. Release*, 2011, **155**, 47-53.
41 Y. Kim, M. H. Pourgholami, D. L. Morris and M. H. Stenzel, *Macromol. Biosci*, 2011, **11**, 219-233.
42 A. Shimoda, S. i. Sawada and K. Akiyoshi, *Macromol. Biosci*, 2011, **11**, 882-888.
43 C. Zhan, B. Gu, C. Xie, J. Li, Y. Liu and W. Lu, *J. Control. Release*, 2010, **143**, 136-142.
44 H. A. Kim, K. Nam and S. W. Kim, *Biomaterials*, 2014, **35**, 7543-7552.
45 W. Song, M. Li, Z. Tang, Q. Li, Y. Yang, H. Liu, T. Duan, H. Hong and X. Chen, *Macromol. Biosci*, 2012, **12**, 1514-1523.
46 H. Uchino, Y. Matsumura, T. Negishi, F. Koizumi, T. Hayashi, T. Honda, N. Nishiyama, K. Kataoka, S. Naito and T. Kakizoe, *Br. J. Cancer*, 2005, **93**, 678-687.
47 C. Deng, H. Y. Tian, P. B. Zhang, J. Sun, X. S. Chen and X. B. Jing, *Biomacromolecules*, 2006, **7**, 590-596.
48 N. Graf, D. R. Bielenberg, N. Kolishetti, C. Muus, J. Banyard, O. C. Farokhzad and S. J. Lippard, *ACS Nano*, 2012, **6**, 4530-4539.



 